GEOS 28600

The science of landscapes:
Earth & Planetary Surface Processes

Lecture 2

Wednesday 3 October 2018

PACIFIC OCEAN BASIN

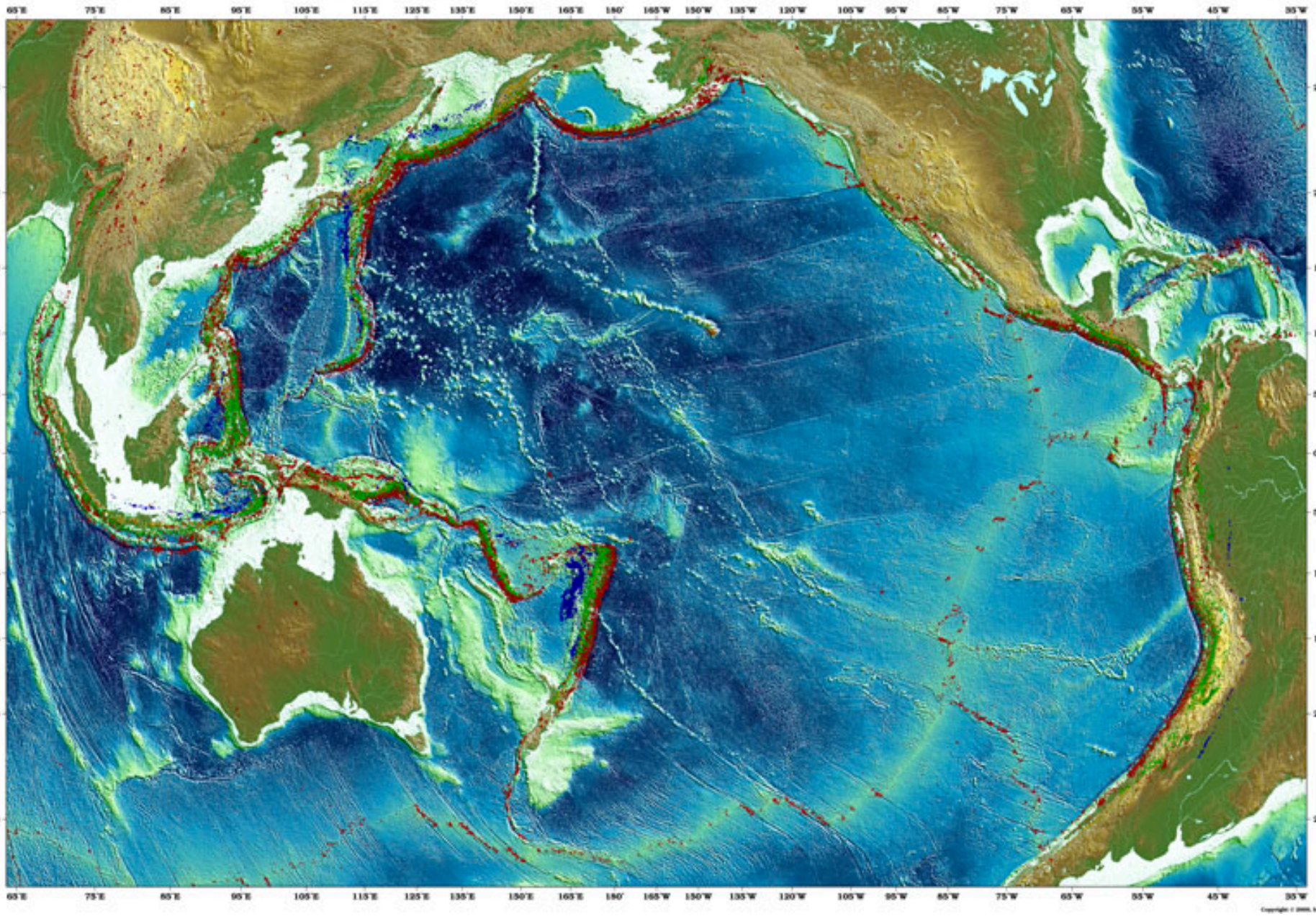

Mapping underwater volcanoes from space

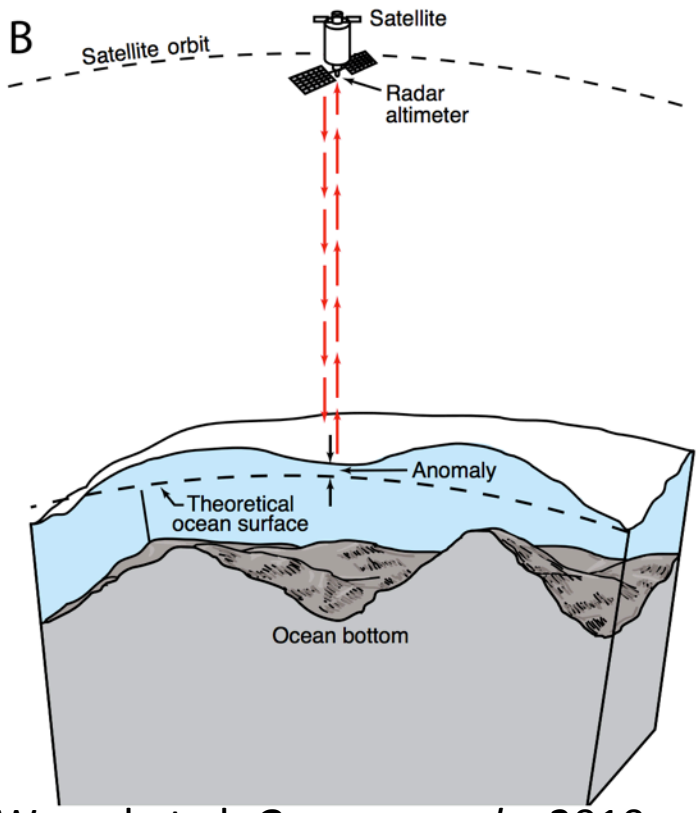

Wessel et al. *Oceanography* 2010

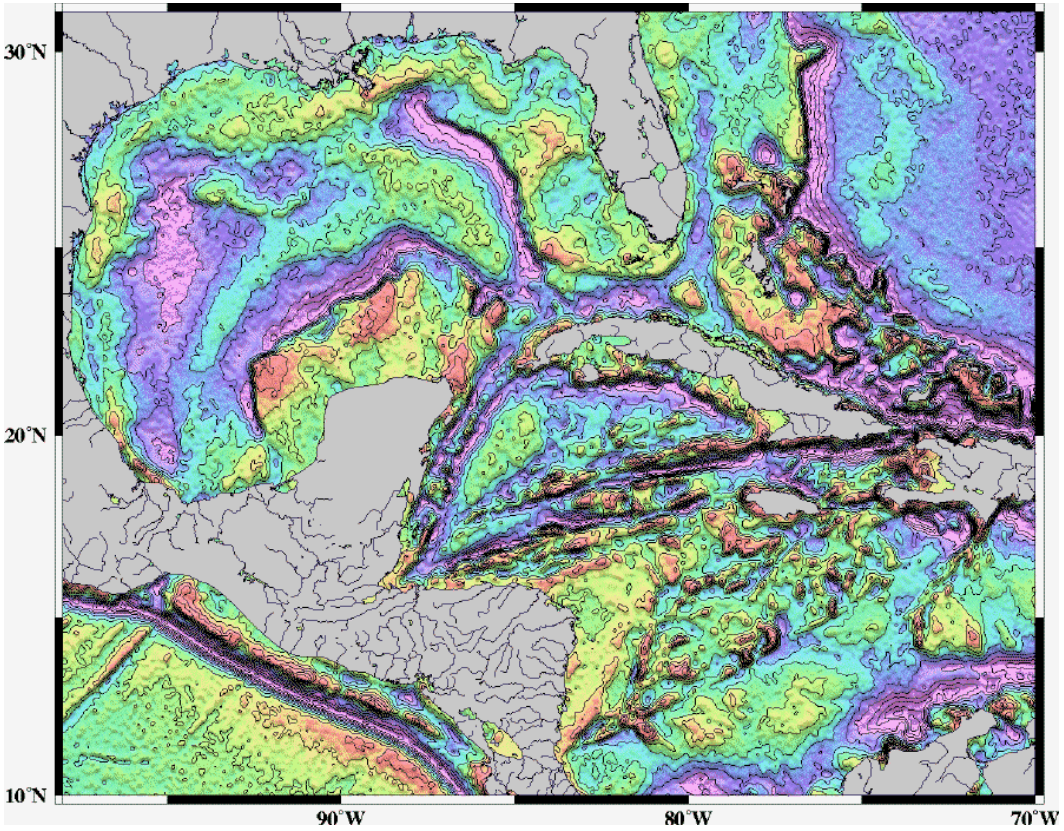

Smith & Sandwell 1997

Most Earth seafloor “bathymetry” is actually inferred from constraints on gravity!

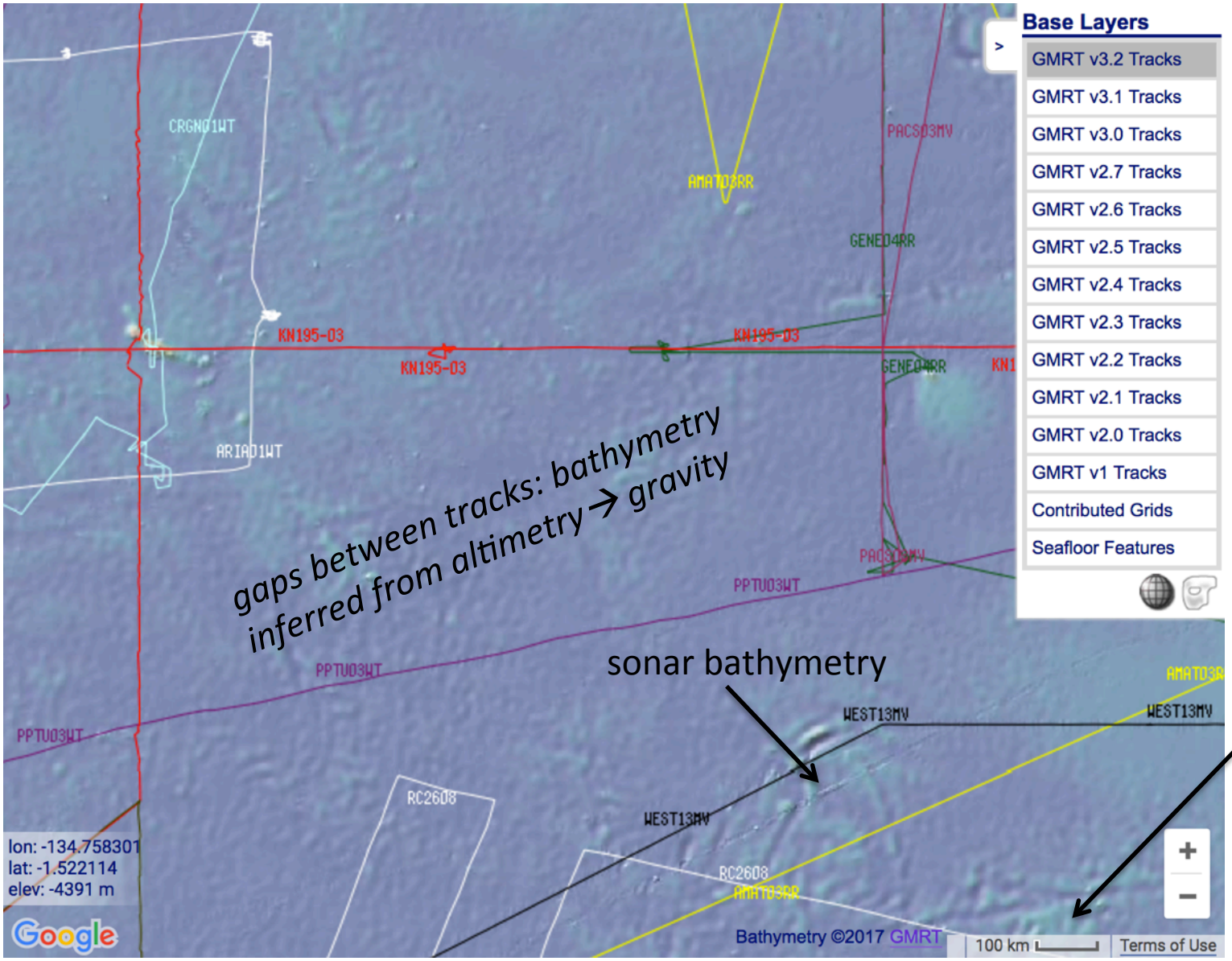

http://www.marine-geo.org/portals/gmrt/

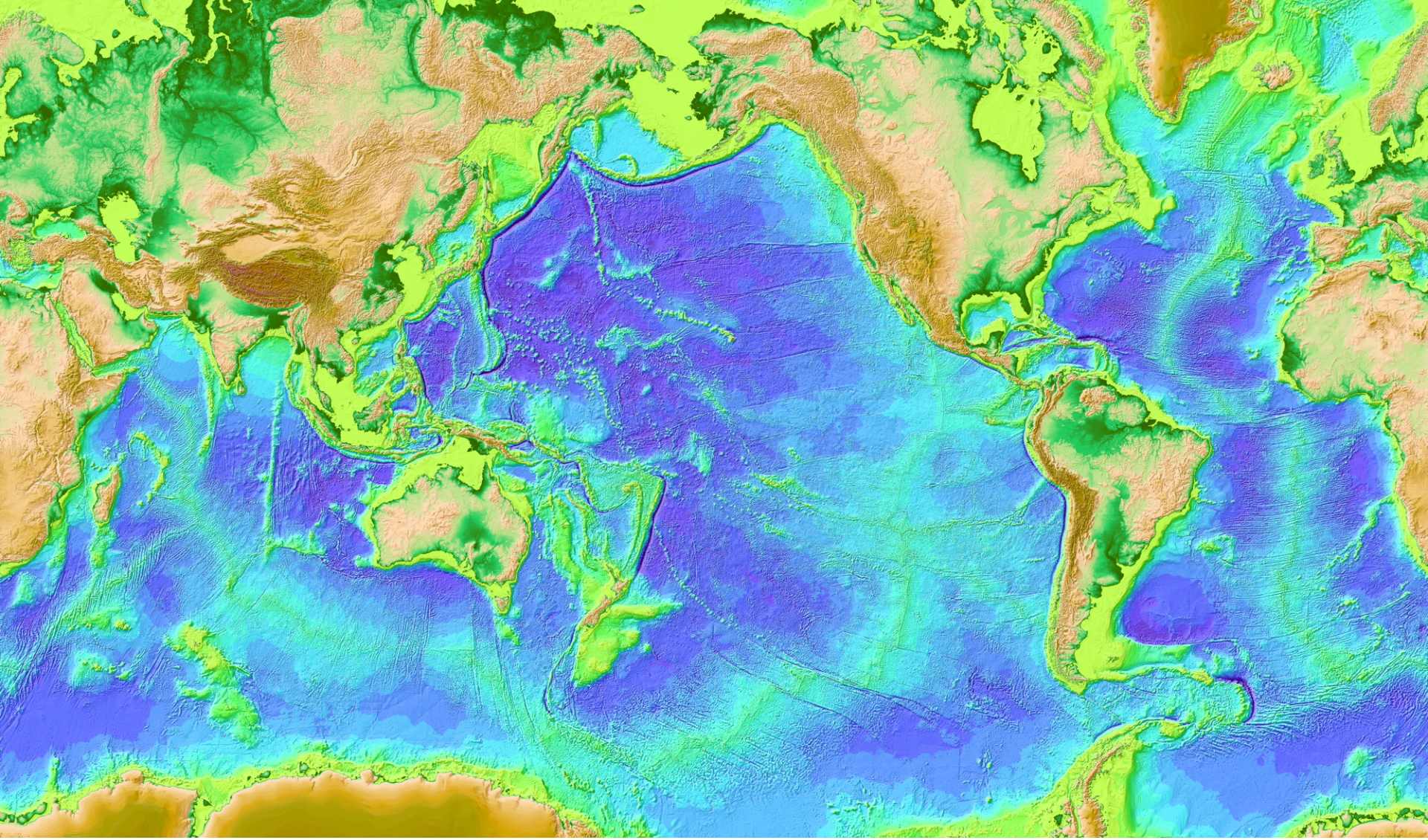

Airy isostasy (floating)

$$[\rho_c t + \rho_m(d_c - t)]g = [\rho_c(t + h_A + t_R) + \rho_m(d_c - t - t_R)]g.$$

$$h_A = \left(\frac{\rho_m - \rho_c}{\rho_c}\right) t_R$$

b)

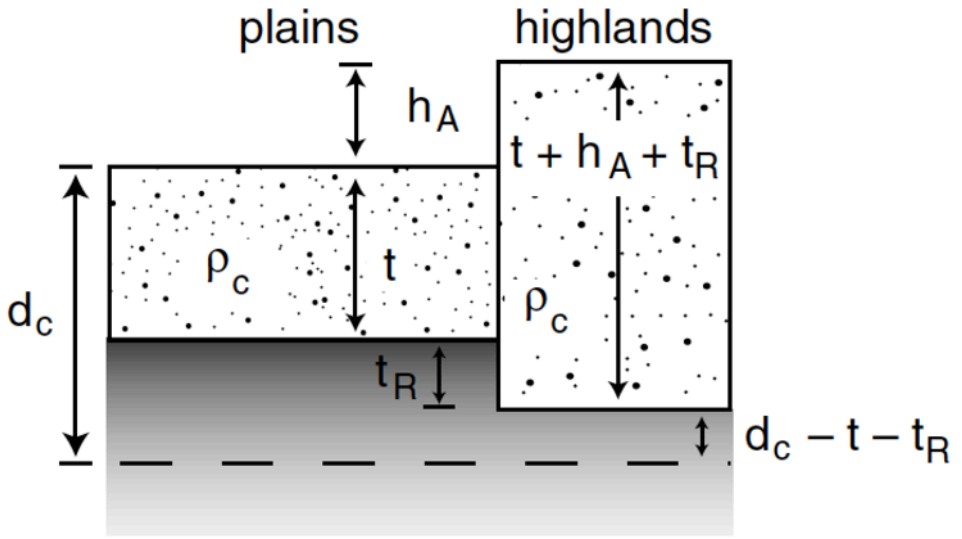

Free-air gravity anomaly is negligibly small for loads small compared to planet radius

Switch to chalkboard

How is topography supported?

WRAP-UP TRUE POLAR WANDER FROM LECTURE 1

REVIEW REQUIRED READING (CHAPTER 2 IN MELOSH)

EXPECTATIONS AND OBSERVATIONS: BOUGUER GRAVITY EQUATION, GRAVITY-TOPOGRAPHY CORRELATION, ADMITTANCE

MECHANISMS: AIRY ISOSTASY, FLEXURE
(MEMBRANE STRESSES)

APPLICATIONS: DENSITY/POROSITY; INFERENCE OF BURIED OCEANS; STRENGTH → HEAT FLOW → THERMAL HISTORY

Key points from today

- principle of true polar wander;
  evidence for true polar wander.

- Relationship between topography & gravity at length scales much larger than, comparable to, and much smaller than, the lithospheric thickness.
- Explanation of Airy isostasy
- Quantities inferred from topography←→gravity comparison.

How is topography supported?

MENTION AN UNSOLVED PROBLEM RAISED BY CHAPTER 2 IN MELOSH

EXPECTATIONS AND OBSERVATIONS: BOUGUER GRAVITY EQUATION, GRAVITY-TOPOGRAPHY CORRELATION, ADMITTANCE

MECHANISMS: AIRY ISOSTASY, FLEXURE

(MEMBRANE STRESSES)

APPLICATIONS: DENSITY/POROSITY; INFERENCE OF BURIED OCEANS; STRENGTH → HEAT FLOW → THERMAL HISTORY

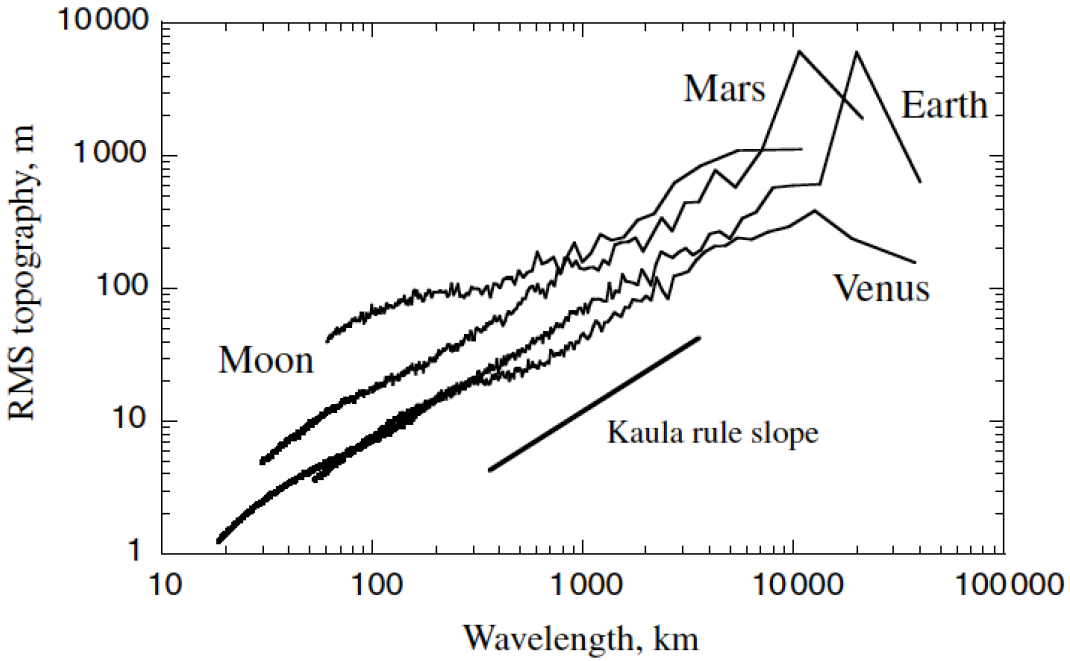

Figure 2.4 Topographic power spectra of the terrestrial planets and the Moon, excluding Mercury for which the necessary data does not yet exist. Lunar spectral data are from the Kaguya data set (Araki *et al.* 2009). Spectral data on Earth, Venus, and Mars are from Mark Wieczorek's website, http://www.ipgp.fr/~wieczor/SH/SH.html, files SRTMP2160, VenusTopo719.shape and MarsTopo719.shape, respectively.

- Unsolved theory problem (Rosenberg, Aharonson & Sari, JGR 2015)
- Matern functions? (Simons et al. AGU 2015)

How is topography supported?

WRAP-UP TRUE POLAR WANDER FROM LECTURE 1

REVIEW REQUIRED READING (CHAPTER 2 IN MELOSH)

EXPECTATIONS AND OBSERVATIONS: BOUGUER GRAVITY EQUATION, GRAVITY-TOPOGRAPHY CORRELATION, ADMITTANCE

MECHANISMS: AIRY ISOSTASY, FLEXURE
(MEMBRANE STRESSES)

APPLICATIONS: DENSITY/POROSITY; INFERENCE OF BURIED OCEANS; STRENGTH → HEAT FLOW → THERMAL HISTORY

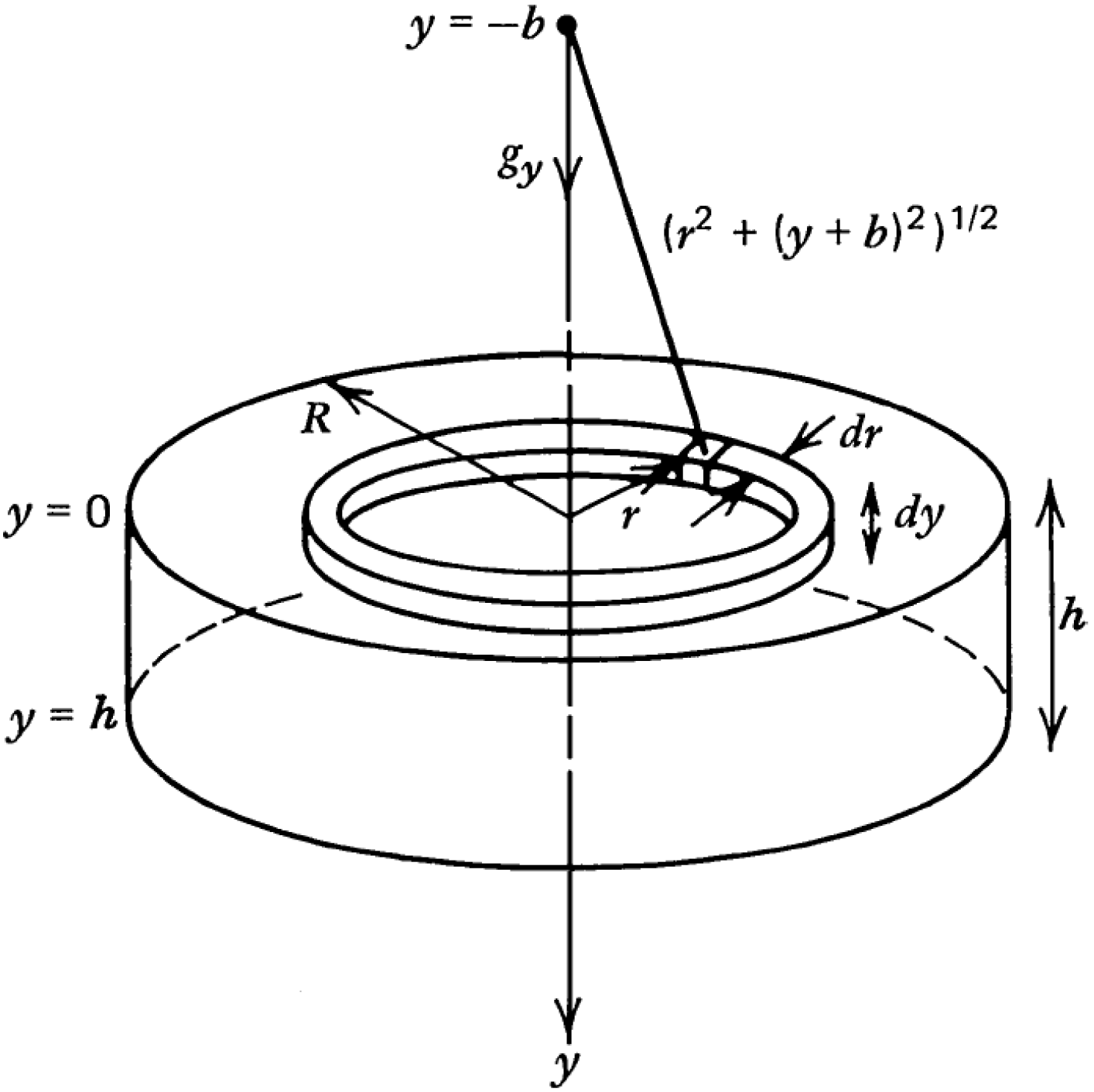
y = −b
g_y
(r² + (y + b)²)^1/2
R
dr
r
dy
y = 0
y = h
h
y

Following Turcotte & Schubert (2nd edn):

$$dg_y = \frac{(2\pi r\, dr\, dy)(\rho)G}{[r^2 + (y+b)^2]} \left\{ \frac{y+b}{[r^2 + (y+b)^2]^{1/2}} \right\}$$

$$g_y = 2\pi G \int_0^h \int_0^R \frac{(b+y) r \rho(y)\, dr\, dy}{[r^2 + (b+y)^2]^{3/2}}.$$

$$g_y = 2\pi G \int_0^h \rho(y) \left(1 - \frac{b+y}{[R^2 + (b+y)^2]^{1/2}} \right) dy$$

$$R \to \infty \quad \boxed{g_y = 2\pi G \int_0^h \rho(y)\, dy}$$

Example: map underwater volcanoes from space

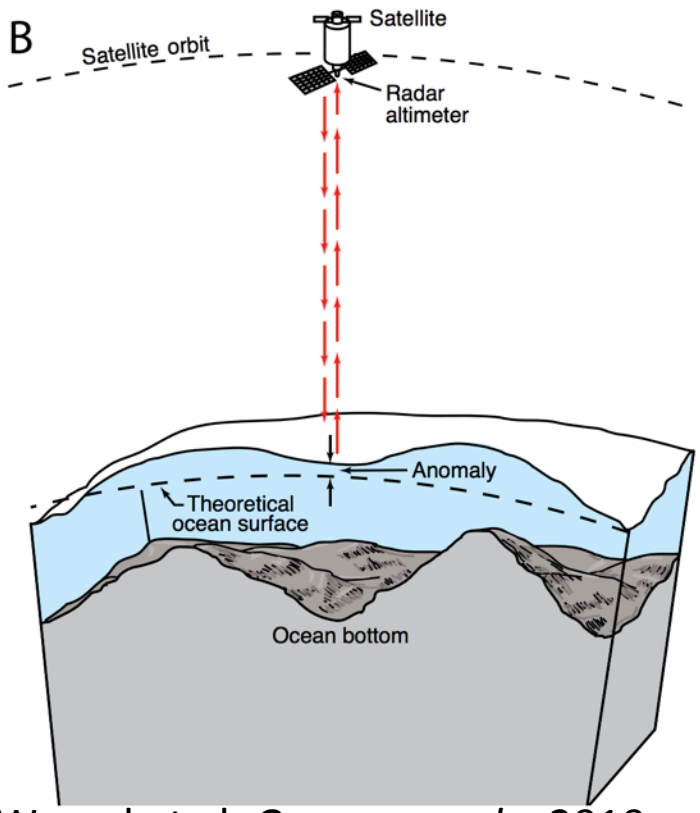

Wessel et al. *Oceanography* 2010

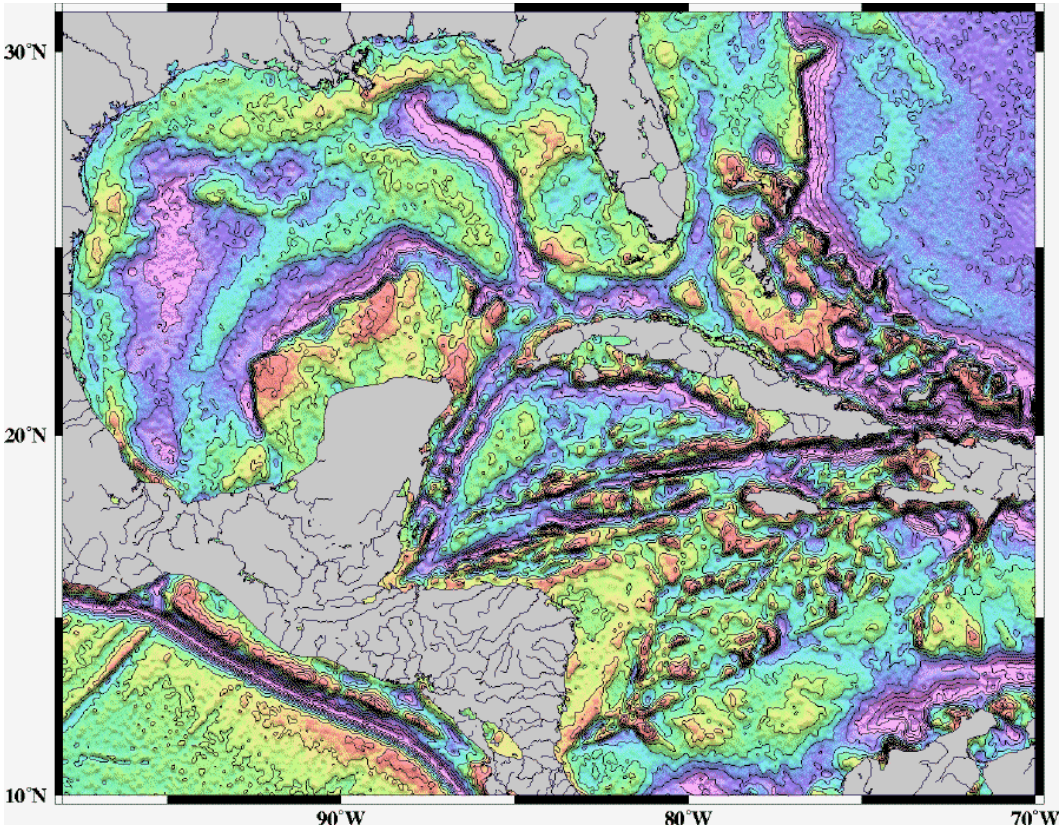

Smith & Sandwell 1997

Most Earth seafloor “bathymetry” is actually inferred from constraints on gravity!

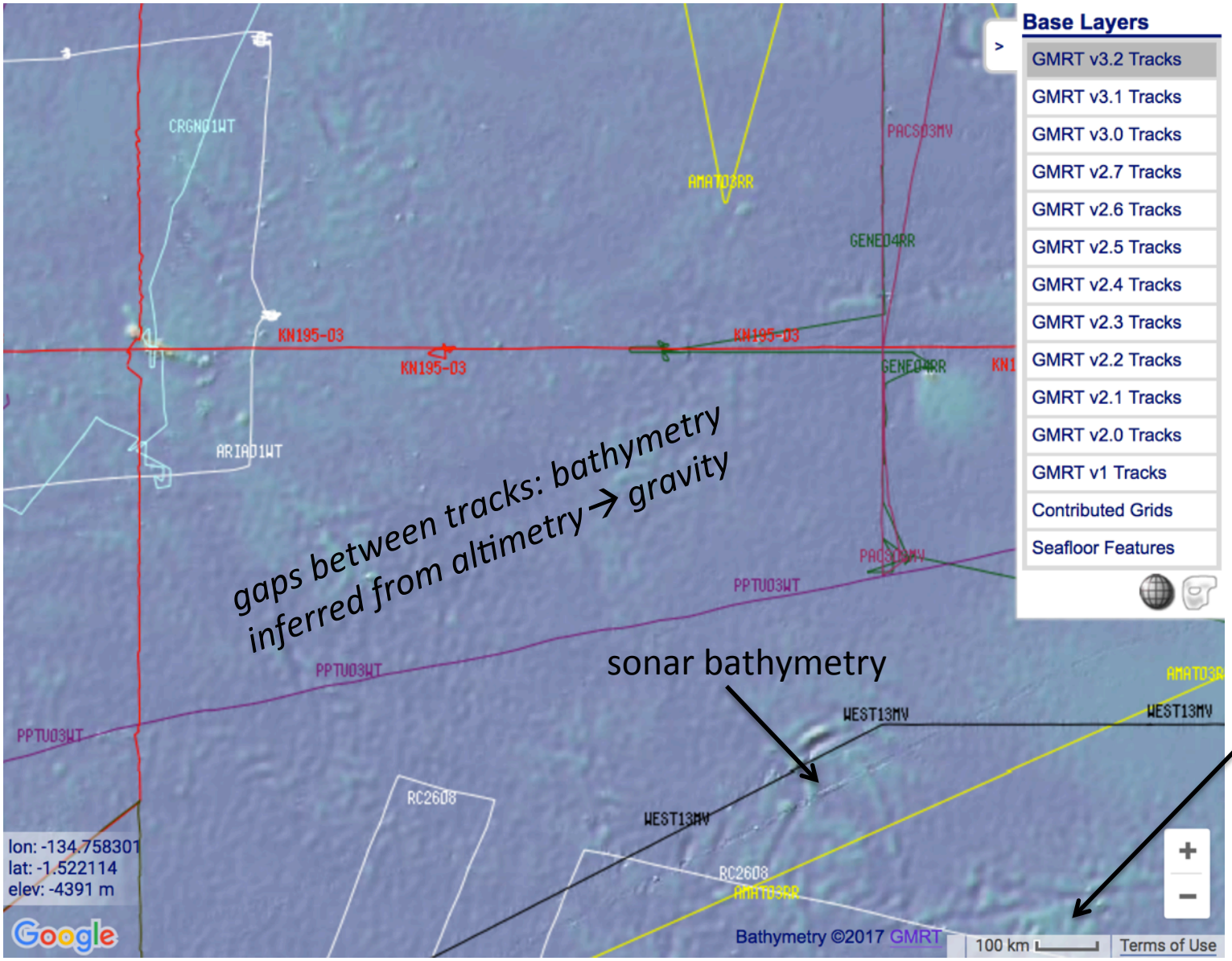

http://www.marine-geo.org/portals/gmrt/

Different worlds show similar behavior in gravity-topography ratio ("admittance") as a function of wavelength

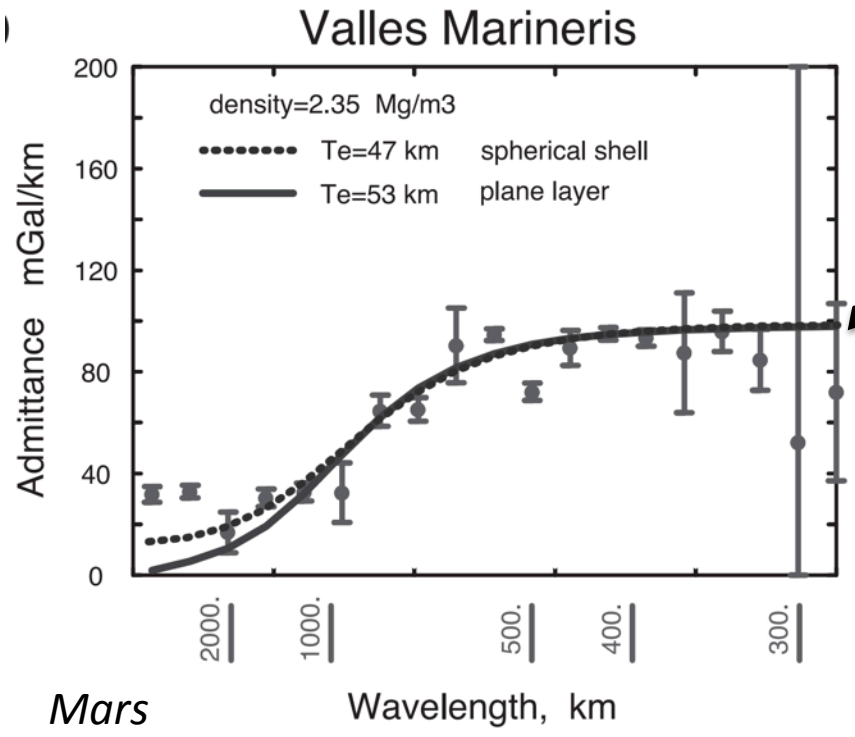

Mars

$2\pi G\rho\Delta z$

Moon

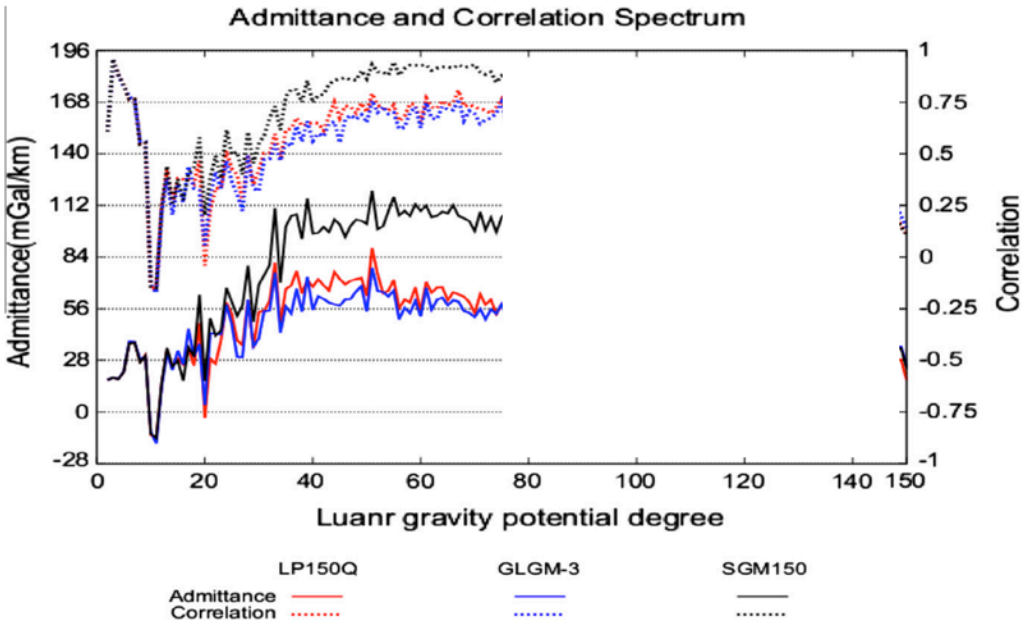

Admittance is sometimes calculated using "Bouguer gravity", gravity that has been corrected for mass of topography

In this course we only use "free-air gravity" (uncorrected for topography).

What is responsible for this support?

How is topography supported?

WRAP-UP TRUE POLAR WANDER FROM LECTURE 1

REVIEW REQUIRED READING (CHAPTER 2 IN MELOSH)

EXPECTATIONS AND OBSERVATIONS: BOUGUER GRAVITY EQUATION, GRAVITY-TOPOGRAPHY CORRELATION, ADMITTANCE

MECHANISMS: AIRY ISOSTASY, FLEXURE
(MEMBRANE STRESSES)

APPLICATIONS: DENSITY/POROSITY; INFERENCE OF BURIED OCEANS; STRENGTH → HEAT FLOW → THERMAL HISTORY

Airy isostasy (floating)

$$[\rho_c t + \rho_m(d_c - t)]g = [\rho_c(t + h_A + t_R) + \rho_m(d_c - t - t_R)]g.$$

$$h_A = \left(\frac{\rho_m - \rho_c}{\rho_c}\right) t_R$$

b)

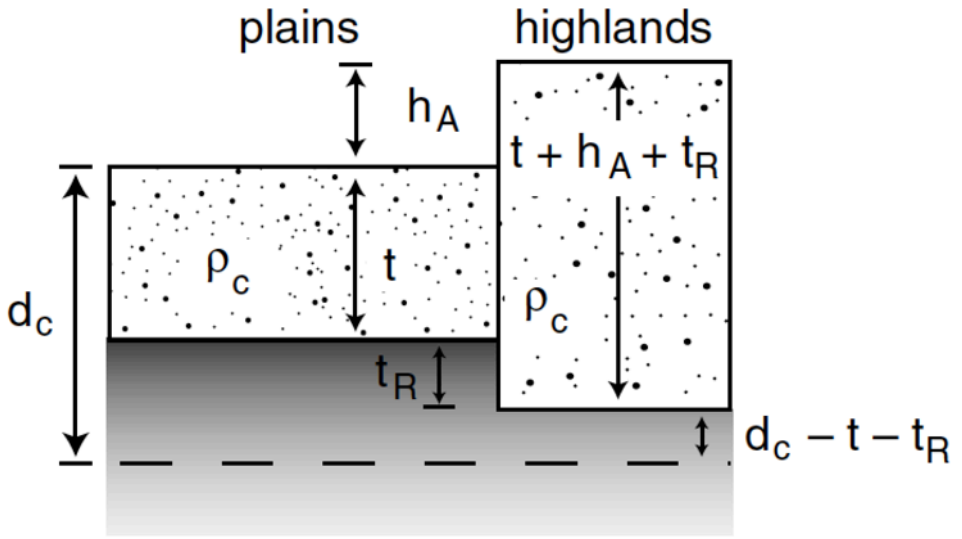

Free-air gravity anomaly is negligibly small for loads small compared to planet radius

Definition of the lithosphere

elastic lithosphere
– supports loads over geologic time

separate from:

seismic lithosphere – permits earthquakes

thermal boundary layer
- layer that is conductively affected by the cold boundary condition of the planet's surface

Watts, in Treatise on Geophysics (1st edn.), 2007

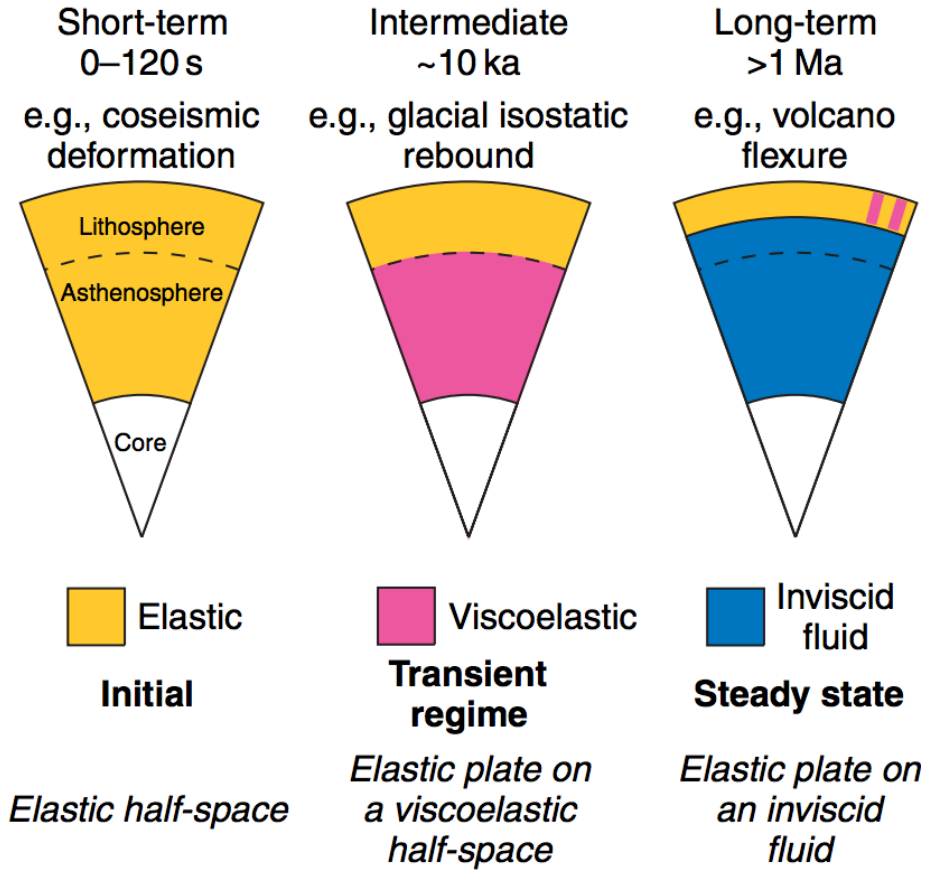

Figure 8 Schematic diagram illustrating how the Earth's outermost layers respond to loads of different timescales. The loads have been arbitrarily divided into: short-term, intermediate, and long-term timescales. Examples of short-term loads include the coseismic deformation associated with earthquake triggering, intermediate loads include glacial isostatic adjustment, and long-term loads include volcano flexure. The bold text at the bottom of the diagram describes the deformation regime corresponding to each load duration. The italic text indicates the most commonly used deformation models at each timescale.

Lithosphere: strength versus depth

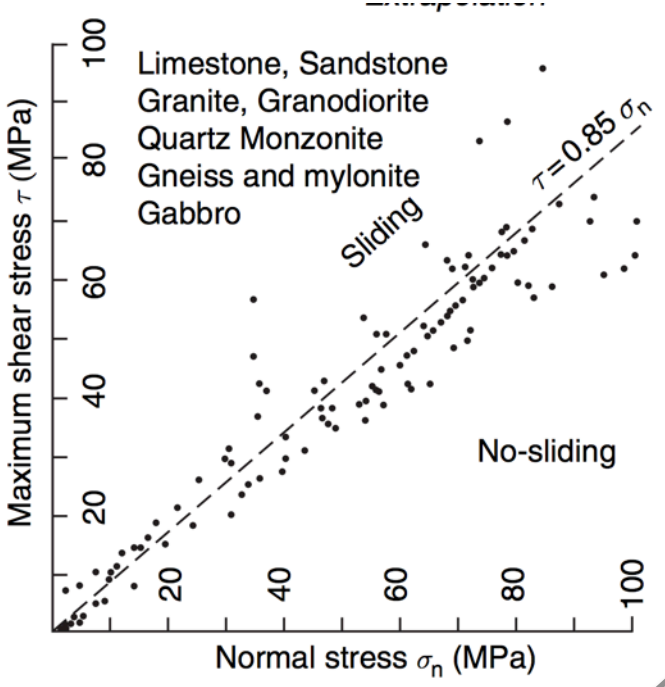

Byerlee's law

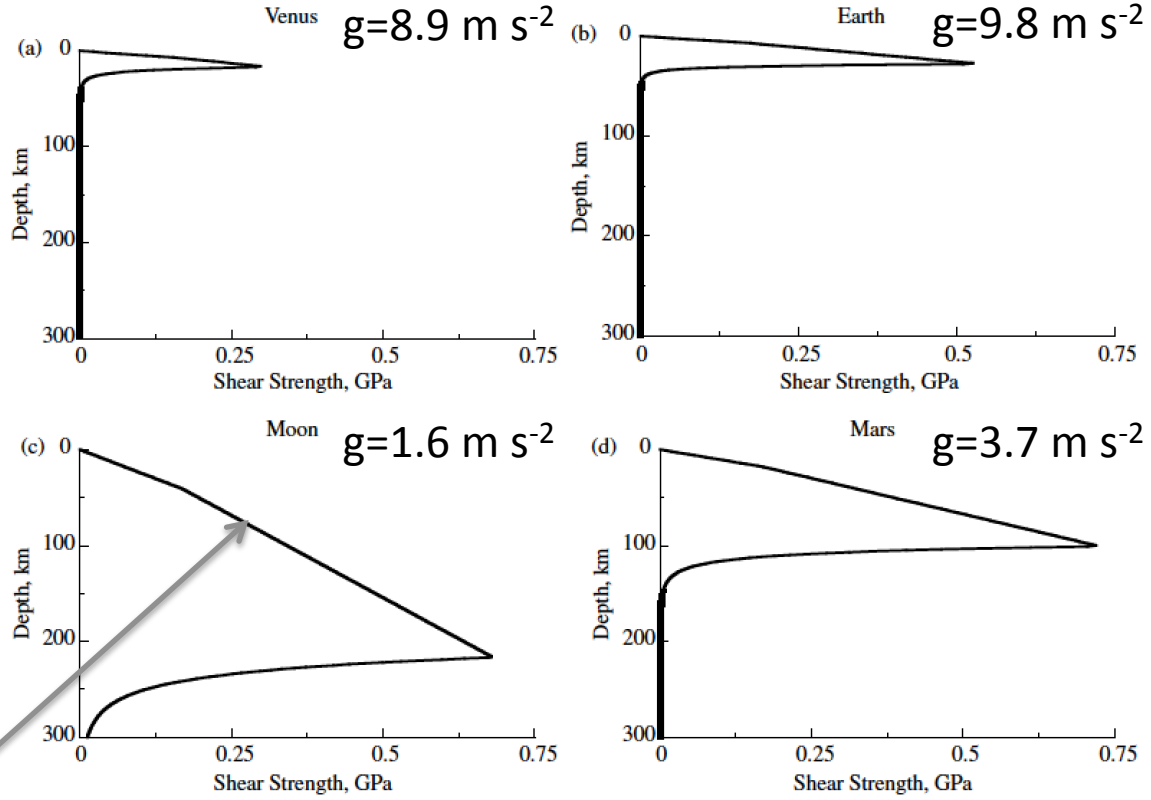

Figure 3.9 Strength profiles for the lithospheres of (a) Venus, (b) the Earth, (c) the Moon, and (d) Mars. The upper parts of the curve are controlled by friction on pre-existing fractures and, thus, follow Byerlee's law, Equation (3.25). The lower portions are cut off by creep in olivine, with parameters listed in Table 3.5. Temperatures are computed from mantle heat flow on the Earth and by assuming an average chondritic composition for the other planets. Thermal conductivity is taken to be 3.0 W/m-K. The strain rate is 10^{-13} s^{-1}, although the curves are only slightly different at 10^{-15} s^{-1}.

stiffness (Pa, N m^{-2})
Young's modulus

elastic thickness (m)

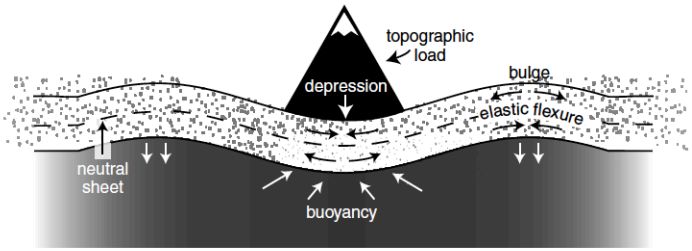

$$D \equiv \frac{Eh^3}{12(1-\nu^2)}$$

flexural rigidity (N m)

Poisson's ratio (0.25 – 0.33, dimensionless)

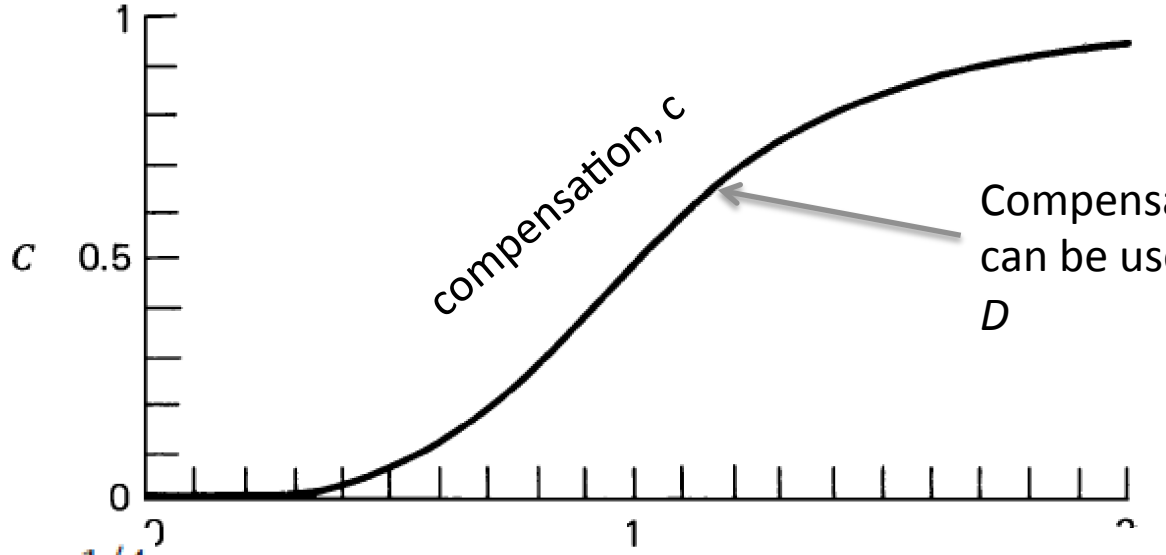

Compensation curves can be used to constrain *D*

wavelength (m)

$$\lambda \ll 2\pi\left(\frac{D}{\rho_c g}\right)^{1/4}$$

$$\frac{\lambda}{2\pi}\left[\frac{g(\rho_m-\rho_c)}{D}\right]^{1/4}$$

$$\lambda \gg 2\pi\left(\frac{D}{\rho_c g}\right)^{1/4}$$

Figure 3.27 Dependence of the degree of compensation on the nondimensional wavelength of periodic topography.

m = [(kg m s^{-2})/(kg m^{-3} × m s^{-2})]$^{1/4}$

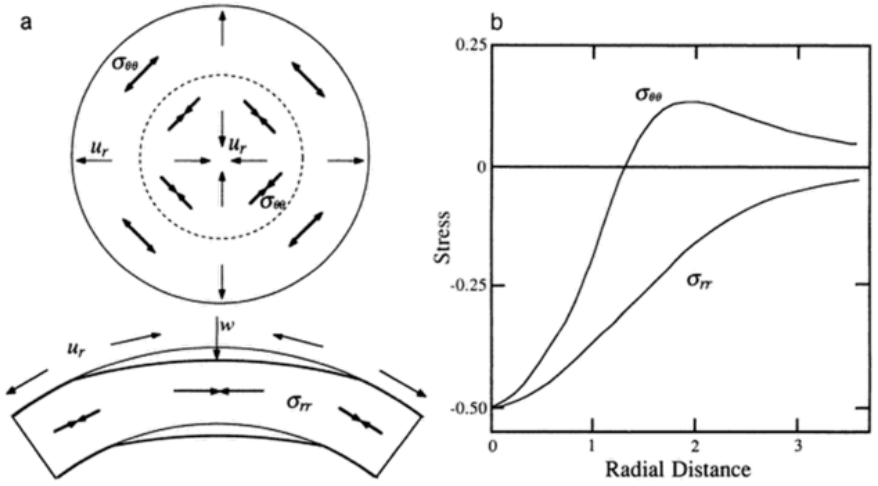

Fig. 2. (a) Schematic diagram of the membrane response of a spherical shell under a long-wavelength load. See Fig. 1 for an explanation of symbols. (b) Profiles of the radial and circumferential membrane stress components for a gaussian load given by $q = q_0 \exp[-(r/r_0)^2]$ on a spherical shell (figure adapted from Turcotte et al. 1981). Radial distance is normalized by r_0 and stress is normalized by $q_0 l_c^2/R$. Tension is positive.

Banerdt et al., ch. in
Kieffer et al. (eds). "Mars", 1992

A different technique is needed for loads with wavelength comparable to the radius of the planet (consider **membrane stresses**)

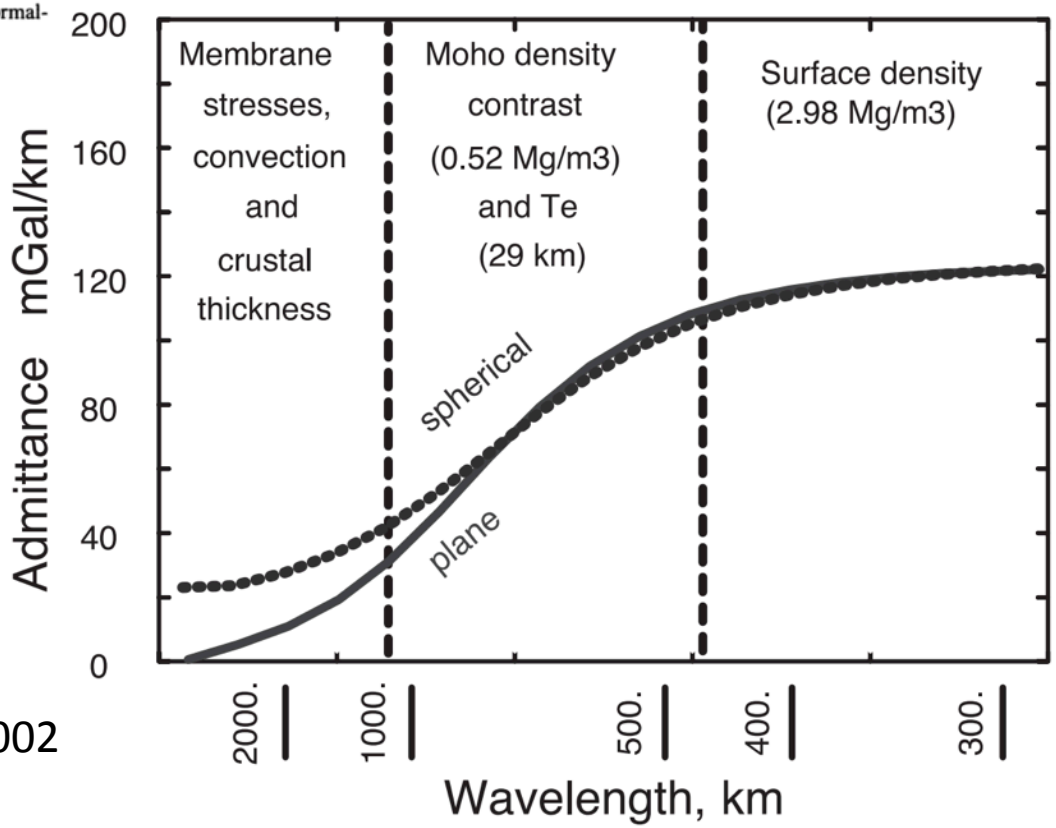

McKenzie et al. EPSL 2002

Membrane support example: Tharsis (volcanic province) load on Mars

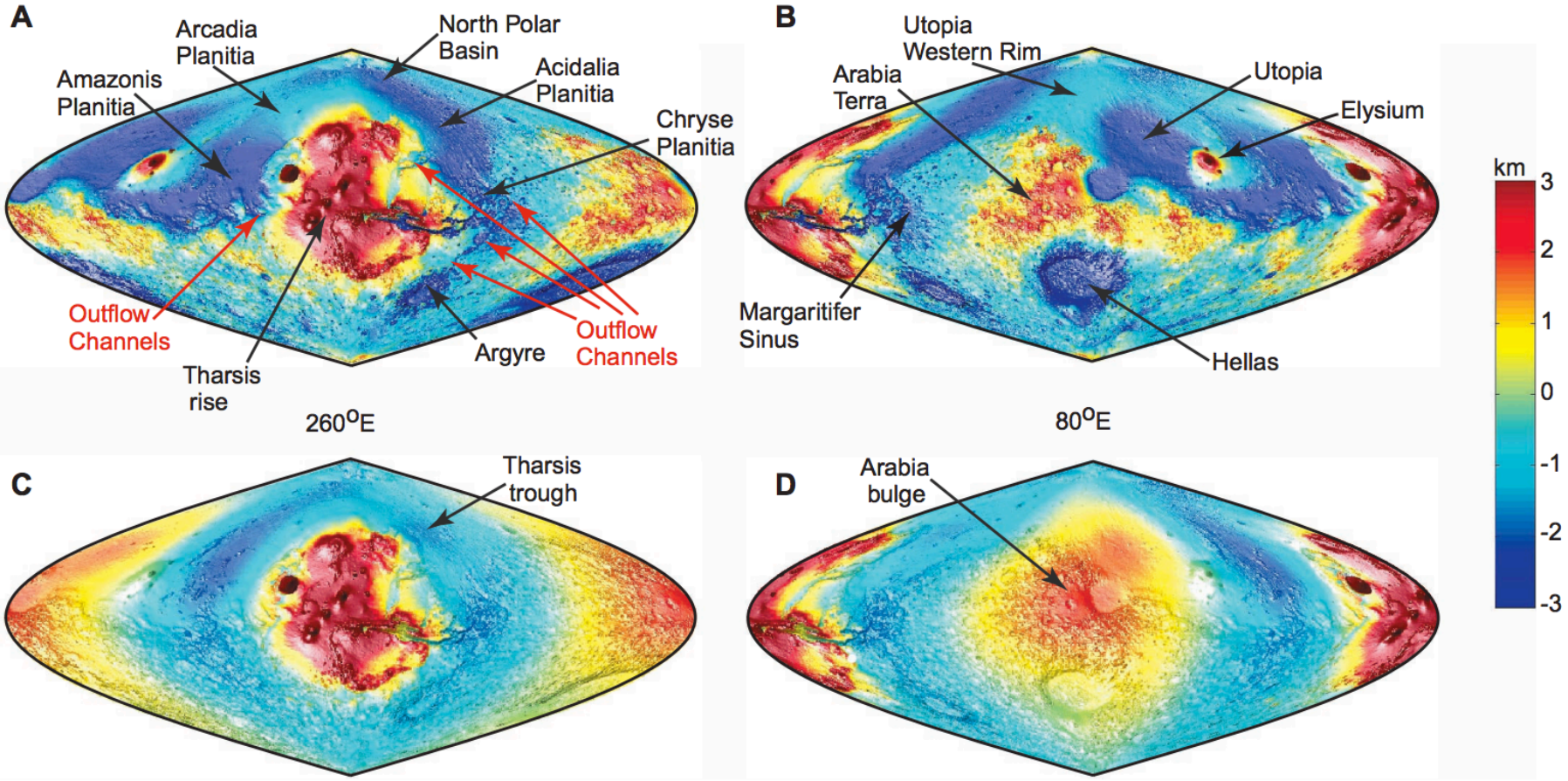

Fig. 3. Observed martian topography displayed for (**A**) the Tharsis and (**B**) the anti-Tharsis hemispheres compared with modeled topography (to $l = 120$) for (**C**) the Tharsis and (**D**) the anti-Tharsis hemispheres. For the model, actual topography is shown in the Tharsis region. All figures are draped over a 3D view of shaded relief.

Phillips et al. Science 2001

How is topography supported?

WRAP-UP TRUE POLAR WANDER FROM LECTURE 1

REVIEW REQUIRED READING (CHAPTER 2 IN MELOSH)

EXPECTATIONS AND OBSERVATIONS: BOUGUER GRAVITY EQUATION, GRAVITY-TOPOGRAPHY CORRELATION, ADMITTANCE

MECHANISMS: AIRY ISOSTASY, FLEXURE
(MEMBRANE STRESSES)

APPLICATIONS: DENSITY/POROSITY; INFERENCE OF BURIED OCEANS; STRENGTH → HEAT FLOW → THERMAL HISTORY

Hydrology of megabreccia: permeability = ? porosity = ?

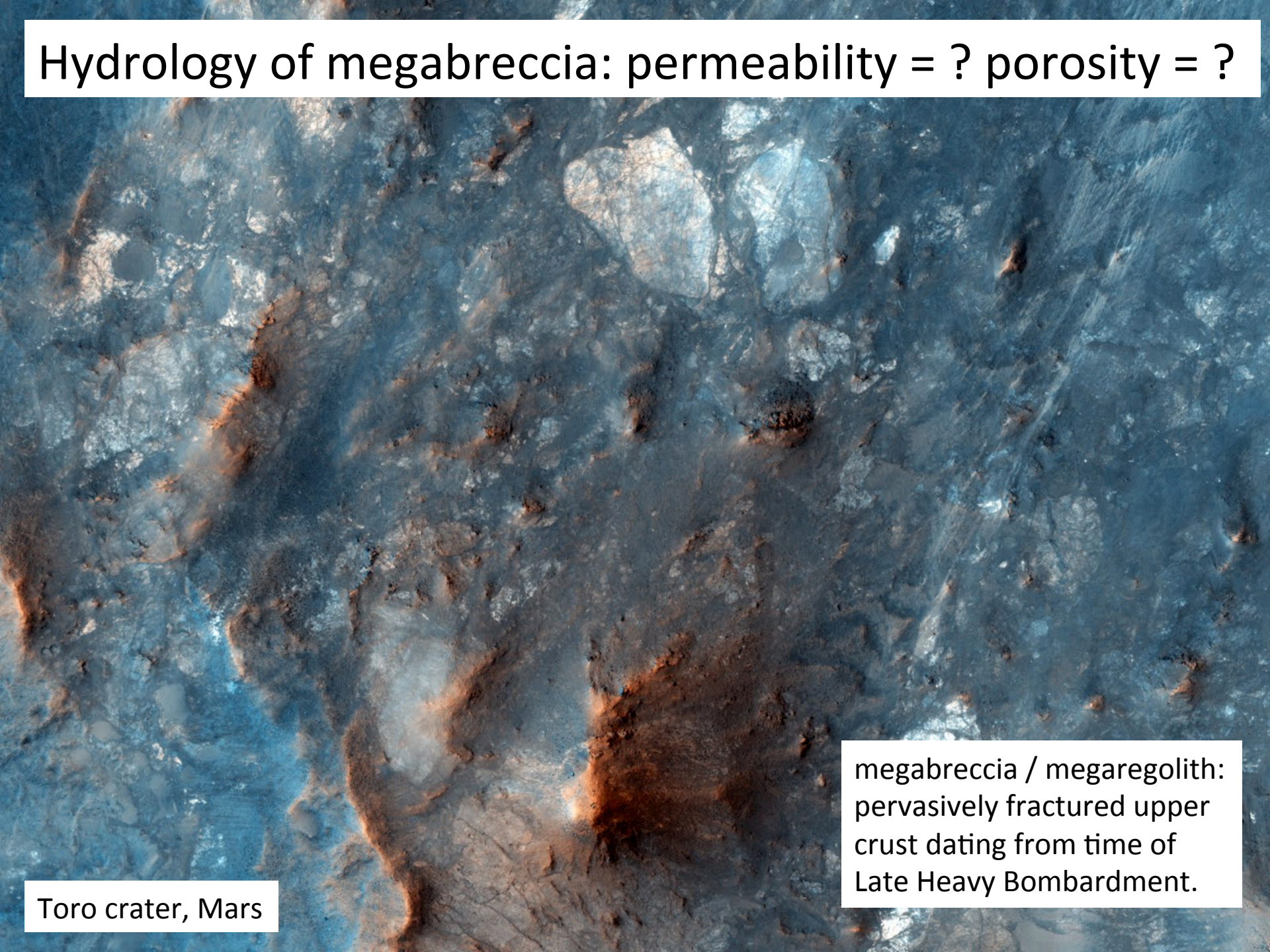

megabreccia / megaregolith: pervasively fractured upper crust dating from time of Late Heavy Bombardment.

Toro crater, Mars

Lunar gravity was poorly mapped before 2010

Problem: how to measure the acceleration of a spacecraft on the far side of the Moon?

Solutions: relay satellite, or two satellites.

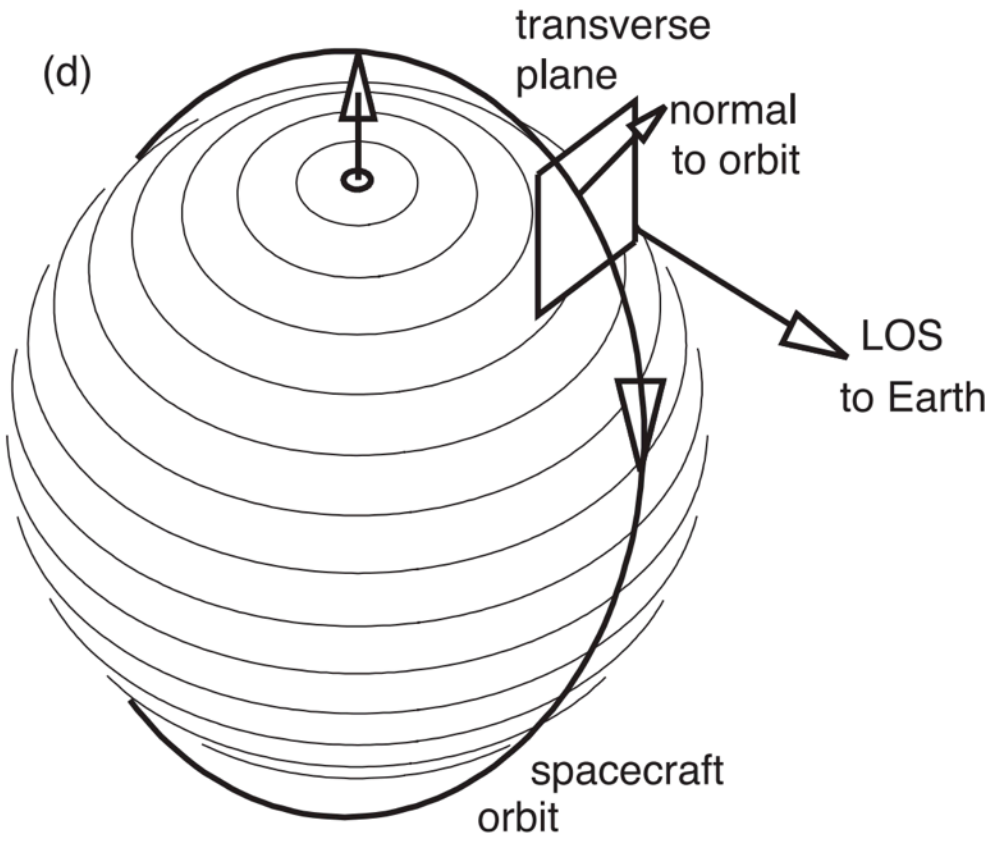

Japan: SELENE mission

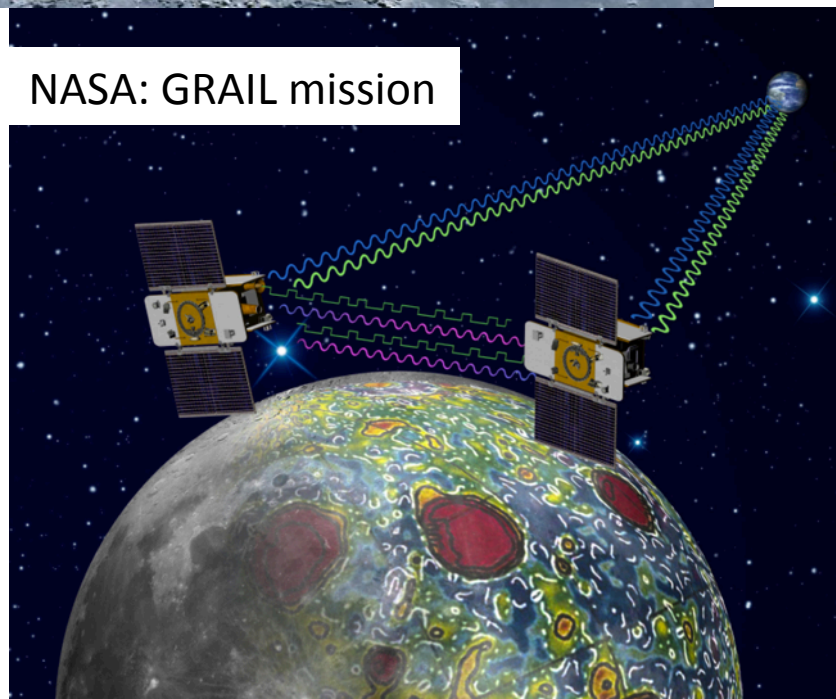

NASA: GRAIL mission

Porosity from gravity-topography ratio

(low flybys possible due to lack of atmosphere on Moon)

Wieczorek et al. Science 2013

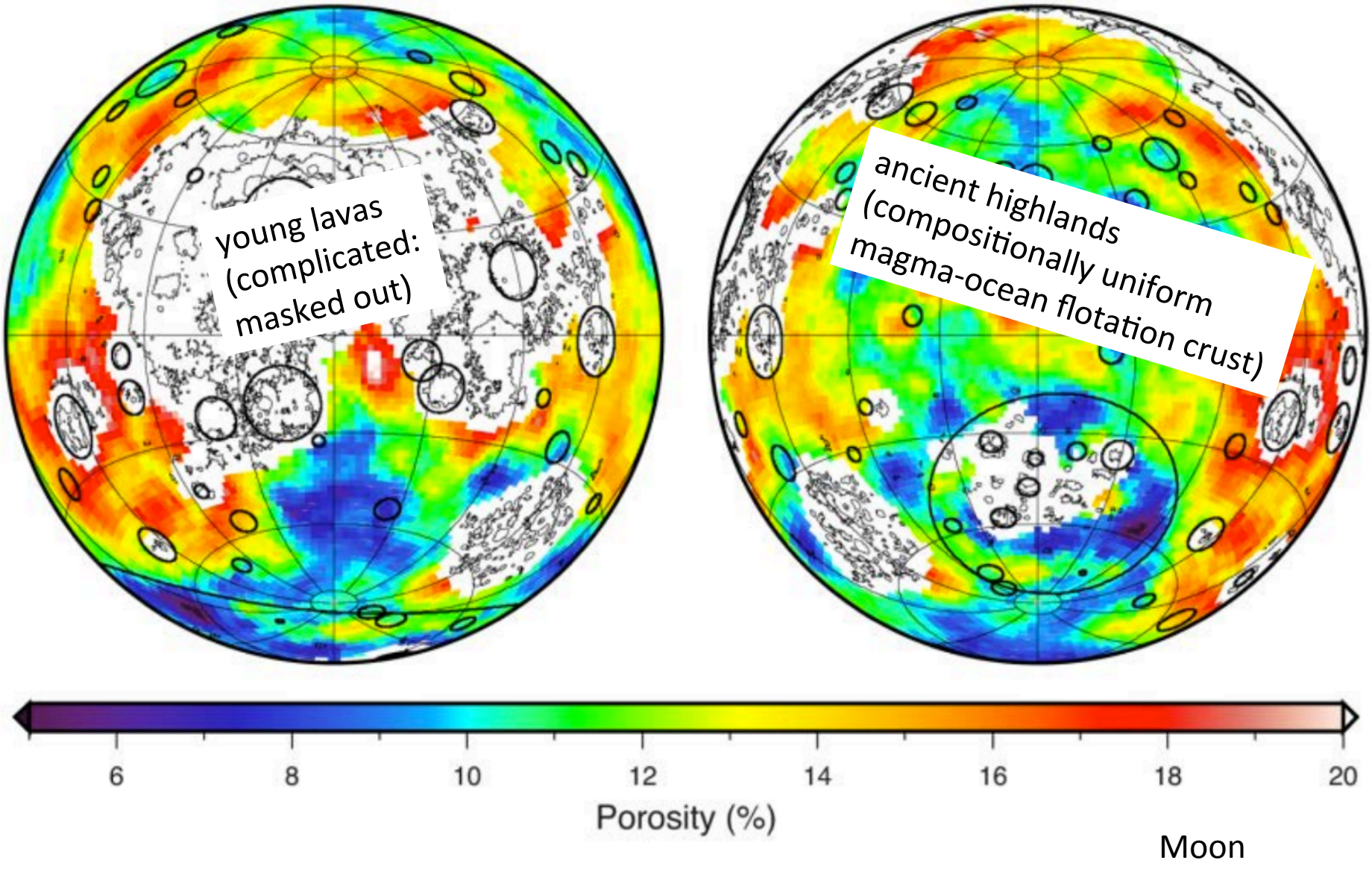

Thermal history of Mars

Base of elastic lithosphere corresponds to T ~ 550-600 C (McNutt, JGR, 1984)

heat flow (W m^{-2})

depth(m)

$$T_z = T_s + \frac{Fz}{k_c}$$

surface T(K)

thermal conductivity (W m^{-1} K^{-1})

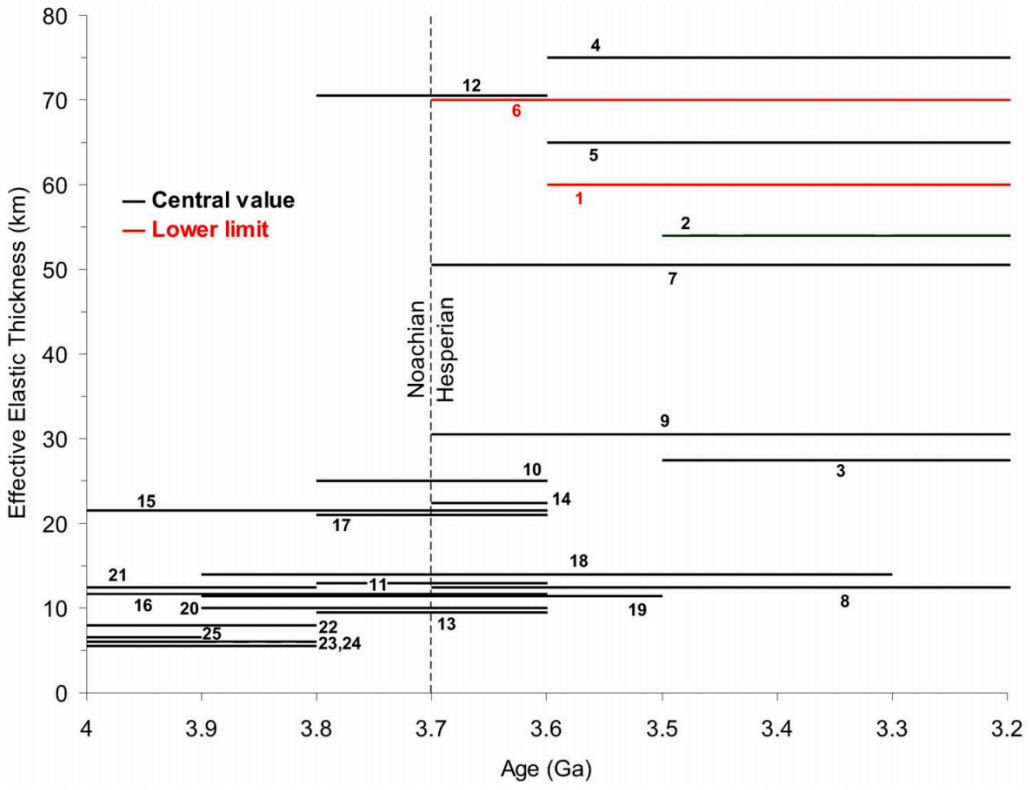

→ Major reduction in Mars' geothermal heat flow at around the time that the surface was drying out.

Figure 3 | Effective elastic thickness of the lithosphere (T_e) for martian terrains loaded (or that could have been loaded) in Noachian or Hesperian times, as a function of age. Numbers referring to given geological features are as in Table 1. For clarity, for a given feature only the central T_e value of the range in Table 1 is shown. Line lengths indicate uncertainty related to loading age.

Ruiz et al., Nature Scientific Reports, 2014

Inferring oceans on Europa

$$D \equiv \frac{Eh^3}{12(1-\nu^2)}$$

Hurford et al. Icarus 2005
Billings & Kattenhorn Icarus 2005

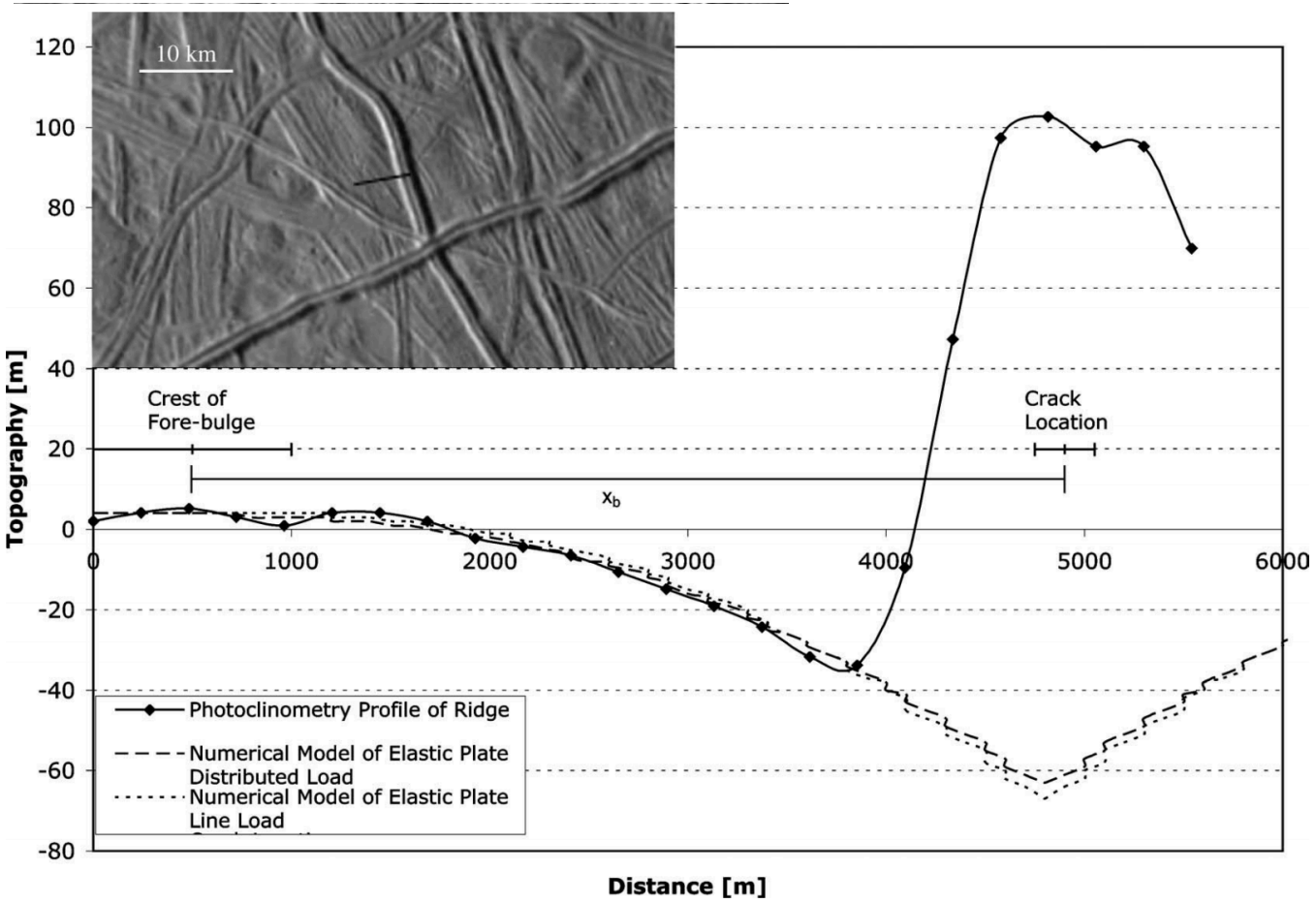

→ Elastic thickness is small
→ Ice is soft and warm at shallow depths
→ (From Europa's overall density) water substance persists to great depth
→ Most of the water is very warm and likely liquid

Key points: topography versus gravity

- Relationship between topography & gravity at length scales much larger than, comparable to, and much smaller than, the lithospheric thickness.
- Explanation of Airy isostasy
- Quantities inferred from topography←→gravity comparison.

Next lecture: topography and tectonics.

Additional slides

Flexure

elastic thickness (m)

$$\alpha = \left[\frac{1}{3(1-\nu^2)} \frac{Et^3}{\rho_m g} \right]^{1/4}$$

flexural parameter

Poisson's ratio

gravity (m/s^2)

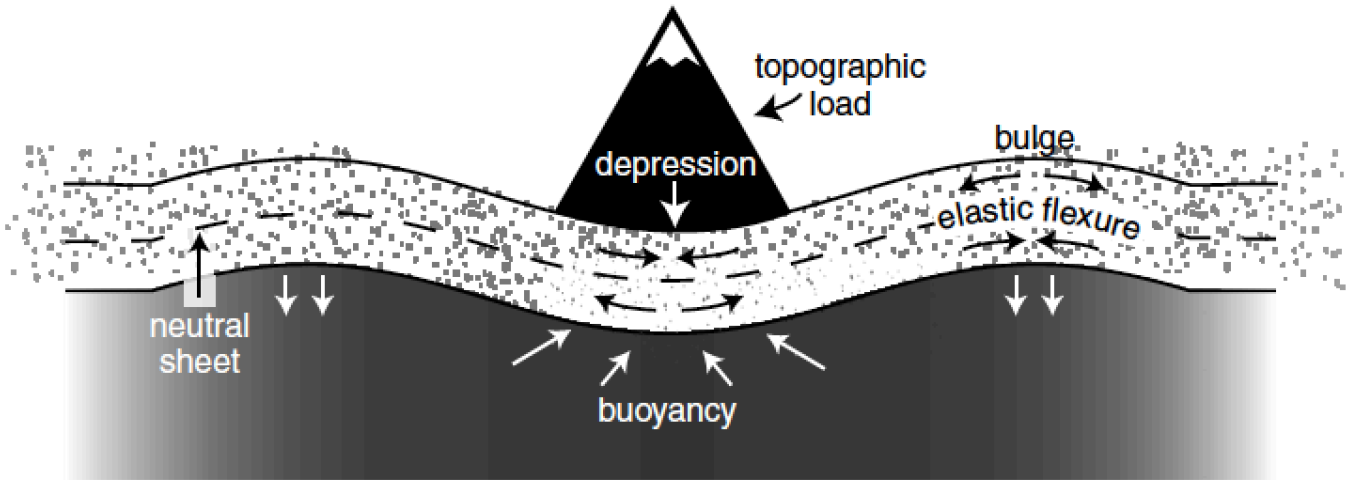

Figure 3.14 Flexure of a floating elastic plate subjected to a topographic load. The weight of the load is supported by a combination of flexural stresses developed by bending of the plate and buoyancy generated by the depression of the lithosphere into the fluid mantle below. This schematic drawing indicates the neutral sheet in the plate by a dashed line.

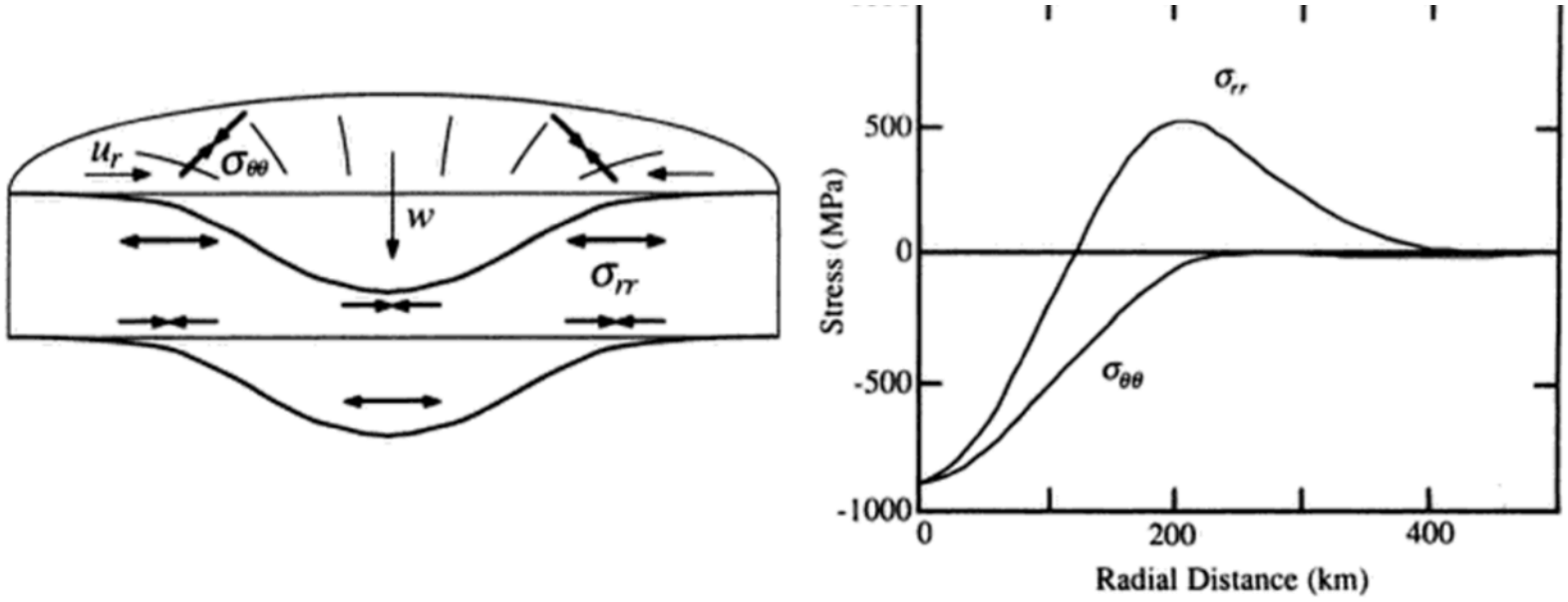

Fig. 1. (a) Schematic diagram of the behavior of a flat plate under an axisymmetric load. Dark arrows denote radial (σ_{rr}) and tangential ($\sigma_{\theta\theta}$) stresses (converging arrows represent compression, diverging arrows extension) and lighter arrows denote radial (u_r) and vertical (w) displacements. (b) Radial profiles of the stress from a local conical load on a shallow shell. The figure is adapted from Comer et al. (1985), who calculated the response of a 22-km-thick Martian elastic lithosphere ($E = 10^{11}$ nt m^{-2}, $\nu = 0.25$, $\Delta\rho = 3.5$ Mg m^{-3}) to a 200-km-

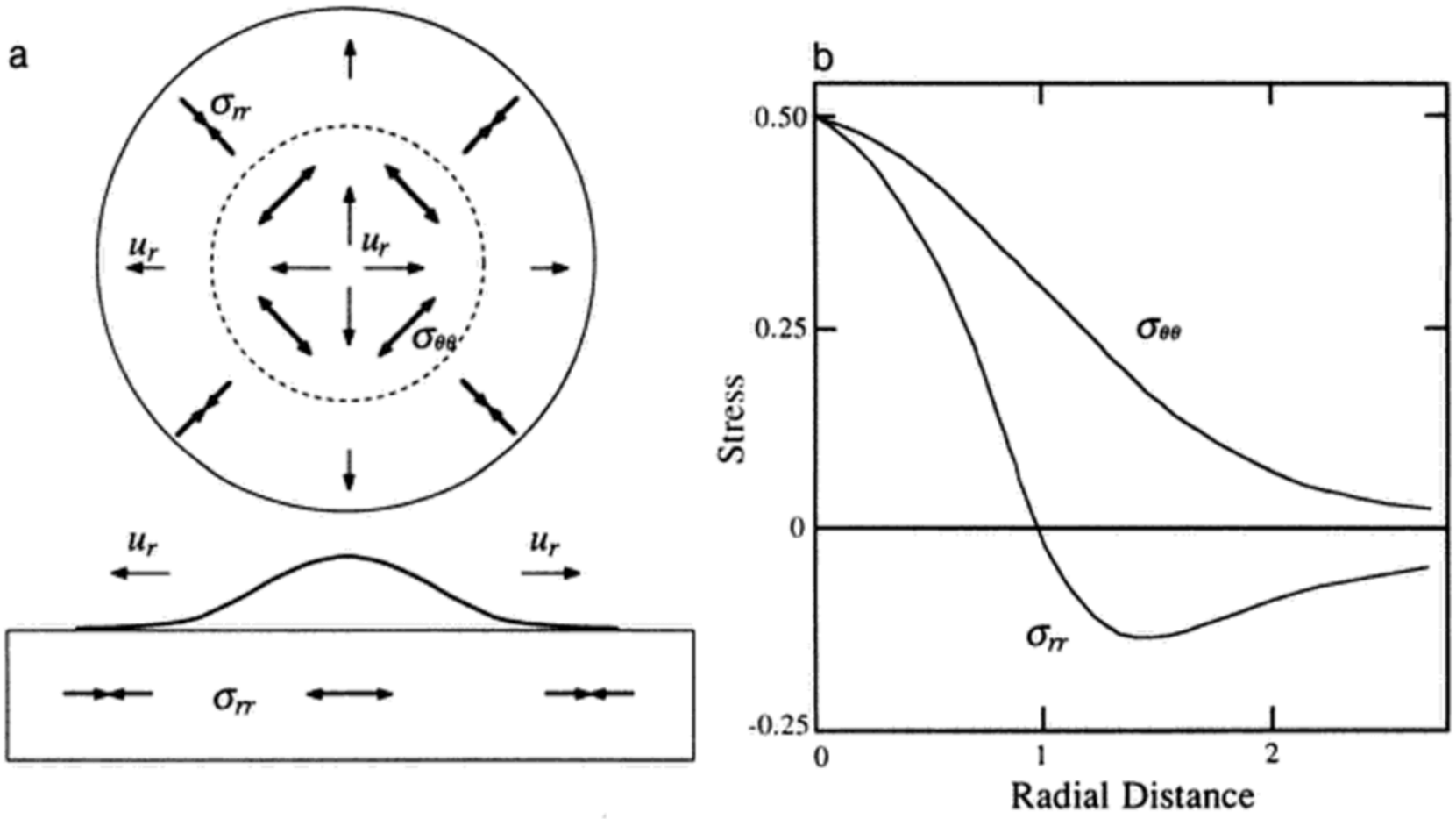

Fig. 3. (a) Schematic diagram of the response of a plate or shell to an isostatic, or gradient load. See Fig. 1 for an explanation of symbols. (b) Generalized profiles of the radial and circumferential membrane stress components for a regional isostatic load. Stress is normalized by $\rho g h_{max}$ and distance is normalized by load radius. Tension is positive.